Analog to electromagnetically induced transparency and Autler-Townes effect demonstrated with photoinduced coupled waveguides

Charles Ciret,[1,2,*] Massimo Alonzo,[1,2] Virginie Coda,[1,2] Andon A. Rangelov,[3] and Germano Montemezzani[1,2]
[1]*Université de Lorraine, LMOPS, EA 4423, 2 rue E. Belin, F-57070 Metz, France*
[2]*Supélec, LMOPS, EA 4423, 2 rue E. Belin, F-57070 Metz, France*
[3]*Department of Physics, Sofia University, 5 James Bourchier Boulevard, 1164 Sofia, Bulgaria*
(Received 24 May 2013; published 25 July 2013)

It is shown that light transfer between two evanescently coupled optical waveguides can be interrupted when strong interaction with a third waveguide is induced. In the strong-interaction regime the transfer can be reactivated upon proper detuning of the waveguide propagation constants. These phenomena can be easily understood using the analog of Autler-Townes splitting and electromagnetically induced transparency from atomic physics. Experimental demonstration is provided using photoinduced reconfigurable waveguides.

DOI: 10.1103/PhysRevA.88.013840 PACS number(s): 42.79.Gn, 42.50.Xa, 42.50.Gy, 42.65.Hw

I. INTRODUCTION

The analogies between wave optics and quantum mechanics are as old as quantum mechanics itself; they served as a source of understanding and development of quantum physics in the pioneering works of de Broglie [1] and Schrödinger [2]. After the full development of quantum mechanics, the analogies have been going in the opposite direction: some of the very well known techniques from coherent quantum control of atoms and molecules found analogs in the realm of optical physics. Examples include the analogies found for Rabi oscillations [3], Landau-Zener tunneling [4–8], and stimulated Raman adiabatic passage (STIRAP) [9–14]. The number of quantum-optical analogies appearing in the literature is still growing rapidly, as described recently in a comprehensive review with a special focus on the use of waveguide structures [15].

Another important quantum effect that holds a direct analogy with classical optical systems is electromagnetically induced transparency (EIT) [16–18]. Different EIT-like optical systems have been demonstrated or proposed on the basis of coupled-ring-resonator resonant cavities [19–21], of electrically controlled periodically poled lithium niobate [22], and of metamaterials [23]. Possible applications for photonic switches [24] or photonic logic [25] inspired by EIT have also been proposed.

In the present work we demonstrate theoretically and experimentally that an even much simpler optical system, composed uniquely of three evanescently coupled straight waveguides, can behave in a way which is analogous to EIT. Moreover, by properly mutually detuning the propagation constants in the waveguides, we demonstrate that a waveguide array can display functionalities analogous to the Autler-Townes effect [26] (ac Stark effect). Section II gives the theoretical background and explains the relationship between the waveguide structure and a coupled three-level quantum system in atomic physics. Section III presents and discusses the experiments performed by means of photoinduced reconfigurable and tunable waveguide structures [27] in a photorefractive material. The experimental results are shown to be in very good agreement with the theory and confirm the expectations.

II. APPROACH AND THEORETICAL BACKGROUND

The optical system used to demonstrate the equivalence with the EIT and the Autler-Townes effect is shown in Fig. 1 and consists of three closely spaced planar-type optical waveguides. Initially, light is injected into input waveguide 1 (WG 1). We suppose that, if desired, the refractive index contrast of this waveguide could be changed with respect to the one of the other two waveguides, which leads to a change of the longitudinal propagation constant of the guided wave by an amount $\Delta\beta$ with respect to the common propagation constant β_0 in waveguides 2 and 3 [Fig. 1(b)]. In the paraxial approximation the propagation of a monochromatic light beam in this kind of structure can be described in the framework of the coupled-mode theory (CMT) for which the problem is treated in a discrete way by involving the evanescent coupling between nearest neighbors [28,29]. The corresponding evolution of the wave amplitudes can be described by a set of three coupled differential equations (in matrix form) [15],

$$i\frac{d\mathbf{A}(z)}{dz} = \mathbf{H}(z)\mathbf{A}(z), \tag{1}$$

which has the form of a Schrödinger equation and where the vector $\mathbf{A} = (A_1(z), A_2(z), A_3(z))^T$ contains the amplitudes of the fundamental mode in the individual waveguides.

The matrix $\mathbf{H}$ describes the interaction between the waveguide modes. For the case where WG 2 and WG 3 are identical (propagation constants $\beta_2 = \beta_3 \equiv \beta_0$) and differ from WG 1 (propagation constant $\beta_1 = \beta_0 + \Delta\beta$) we have [28,29]

$$\mathbf{H}(z) = \begin{pmatrix} 0 & C_{1,2}e^{i\Delta\beta z} & 0 \\ C_{2,1}e^{-i\Delta\beta z} & 0 & C_{2,3} \\ 0 & C_{2,3} & 0 \end{pmatrix}. \tag{2}$$

Note that in general the coupling constants for the two different waveguides are unequal ($C_{1,2} \neq C_{2,1}$) [29], while $C_{2,3} = C_{3,2}$, as seen in (2). The term $\Delta\beta$ reflects the propagation velocity mismatch of the wave fronts in waveguides 1 and 2 and takes the role of a detuning.

*charles.ciret@supelec.fr

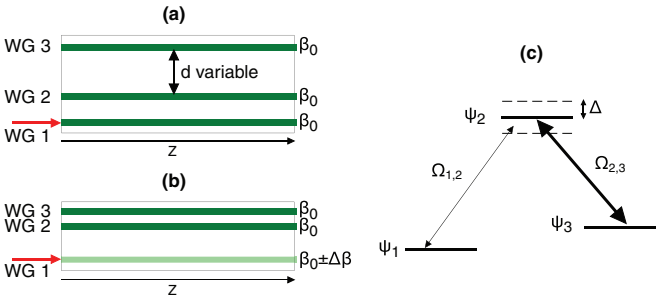

FIG. 1. (Color online) Waveguide configuration for the analogy (a) with EIT, where the distance d between WGs 2 and 3 is variable, and (b) with Autler-Townes effect. In (a) the three waveguides are identical, while in (b) the index contrast of WG 1 differs from that of WG 2 and WG 3, leading to a different longitudinal propagation constant. (c) The equivalent discrete three-level quantum system coupled by coherent fields at or near resonance. $\Omega_{1,2}$ and $\Omega_{2,3}$ are the Rabi frequencies.

Equations (1) and (2) can be brought in a more convenient symmetric and z-independent form by performing the nonunitary transformation $A_1'(z) = \sqrt{C_{2,1}/C_{1,2}}\exp(-i\Delta\beta z)A_1(z)$, $A_2'(z) = A_2(z)$, $A_3'(z) = A_3(z)$, which leads to

$$i\frac{d}{dz}\begin{pmatrix} A_1'(z) \\ A_2'(z) \\ A_3'(z) \end{pmatrix} = \begin{pmatrix} \Delta\beta & C_s & 0 \\ C_s & 0 & C_p \\ 0 & C_p & 0 \end{pmatrix}\begin{pmatrix} A_1'(z) \\ A_2'(z) \\ A_3'(z) \end{pmatrix}, \qquad (3)$$

where $C_s \equiv \sqrt{C_{1,2}C_{2,1}}$ is the geometrical average of the coupling constants between waveguides 1 and 2 in Fig. 1 and $C_p \equiv C_{2,3} = C_{3,2}$ is the coupling constant between waveguides 2 and 3. If we map the longitudinal z dependence into time dependence, Eq. (3) is identical to the time-dependent Schrödinger equation for the three-state Λ system depicted in Fig. 1(c) [30], the role of $\Delta\beta$ being taken by the detuning Δ. In this picture the coupling constant C_s is analogous to the Rabi frequency $\Omega_s \equiv \Omega_{1,2}$ for the signal field that couples states Ψ_1 and Ψ_2, while C_p is associated with the Rabi frequency $\Omega_p \equiv \Omega_{2,3}$ for the pump field that couples states Ψ_2 and Ψ_3.

In the case where the coupling constant C_p between WGs 2 and 3 is much stronger than the averaged coupling constant C_s between WGs 1 and 2, it is natural to diagonalize the strong-coupling portion of the matrix in (3), which leads to an effective two-waveguide system. By defining the new basis

$$\mathbf{B} = \left(A_1', \frac{A_2' + A_3'}{\sqrt{2}}, \frac{A_2' - A_3'}{\sqrt{2}}\right)^T \qquad (4)$$

Eq. (3) is rewritten as

$$i\frac{d}{dz}\begin{pmatrix} B_1(z) \\ B_2(z) \\ B_3(z) \end{pmatrix} = \begin{pmatrix} \Delta\beta & C_s/\sqrt{2} & C_s/\sqrt{2} \\ C_s/\sqrt{2} & C_p & 0 \\ C_s/\sqrt{2} & 0 & -C_p \end{pmatrix}\begin{pmatrix} B_1(z) \\ B_2(z) \\ B_3(z) \end{pmatrix}. \qquad (5)$$

Since, as mentioned above, the three-waveguide system is formally analogous to a three-state Λ system, it should be able to display phenomena equivalent to EIT [16–18,31] and the Autler-Townes effect [26], as discussed next with the help of Eqs. (3) and (5).

Let us first consider the case of three resonant waveguides shown in Fig. 1(a) for which $\Delta\beta = 0$. If WG 3 is far away from WG 2, the coupling constant C_p is weak, $C_p \ll C_s$, and the problem reduces to the one of a directional coupler, for which the light amplitude oscillates sinusoidally between WGs 1 and 2. If the distance between WGs 1 and 2 and refractive index contrasts are chosen such that the length L of the waveguides corresponds to one coupling length, $L = L_c = \pi/(2C_s)$, all the light injected in WG 1 exists in WG 2, so that WG 1 can be considered to be completely opaque to the radiation. This is equivalent to applying a π pulse to an atomic two-level system coupled by a coherent resonant field. The situation changes completely if the coupling C_p is increased by approaching WG 3 towards WG 2 (with the distance between WG 1 and WG 2 being unchanged). In the limiting case where $C_p \gg C_s$, WGs 2 and 3 form a dressed state that prevents the transfer of light from the input WG 1 to WG 2, and WG 1 becomes completely transparent. We can understand the trapping of light in waveguide 1 with the following arguments: the light has two ways of reaching the second waveguide: either directly from WG 1 or via the path WG 1–WG 2–WG 3–WG 2. The latter has comparable probability to the former since C_p is large. Since each transfer from one waveguide to another is associated with a $\pi/2$ phase shift, the amplitudes for these paths exhibit strong destructive interference, and the light is trapped in WG 1. This is true despite the fact that the waveguide length still corresponds to one coupling length between WGs 1 and 2. This phenomenon is analogous to the quantum EIT effect that can be observed in the three-state atomic system of Fig. 1(c) when states Ψ_2 and Ψ_3 are coupled by a strong resonant field. The above arguments are illustrated in Fig. 2, which shows the square of the amplitudes $|A_j'(z)|^2$ (proportional to the peak intensities in the center of waveguide j) for the case $C_p \ll C_s$ [Fig. 2(a)] and for the case $C_p = 5C_s$ [Fig. 2(b)]. The latter case corresponds approximately to the conditions used for the experimental demonstration in the EIT regime discussed in the next section. Note that the slight oscillations observed in Fig. 2(b) disappear completely if the ratio C_p/C_s is increased further (thin red line).

In the case where the transfer of light out of waveguide 1 is inhibited due to the dressed state of WGs 2 and 3, this transfer can be reactivated by detuning the propagation constant in WG 1 by a proper amount $\Delta\beta$ [Fig. 1(b)]. In fact there are two specific values of $\Delta\beta$ for which two of the three diagonal elements in the Hamiltonian matrix of Eq. (5) become equal. For these values, $\Delta\beta = \pm C_p$, propagation in WG 1 becomes resonant with the one either of the mixed state B_2 or of state B_3, which are associated with the fundamental symmetric and antisymmetric supermodes of waveguides 2 and 3, respectively. In essence this resonant coupling is the manifestation of Autler-Townes splitting [26] in our waveguide coupling system. Figure 3(a) illustrates the calculated evolution of the normalized intensities in the three waveguides under the conditions of Fig. 2(b) ($C_p = 5C_s$, thick lines) but for $\Delta\beta = C_p$. Clearly, WG 1 is no longer transparent, and the transfer of light to WGs 2 and 3 is again efficient. As in the previous case, the small oscillations in the evolution disappear if the coupling between states 2 and 3 is increased further (thin lines). It is worth noticing that, as seen in Fig. 3(a), for a normalized distance equal to 1 ($z = L_c$) the transfer is

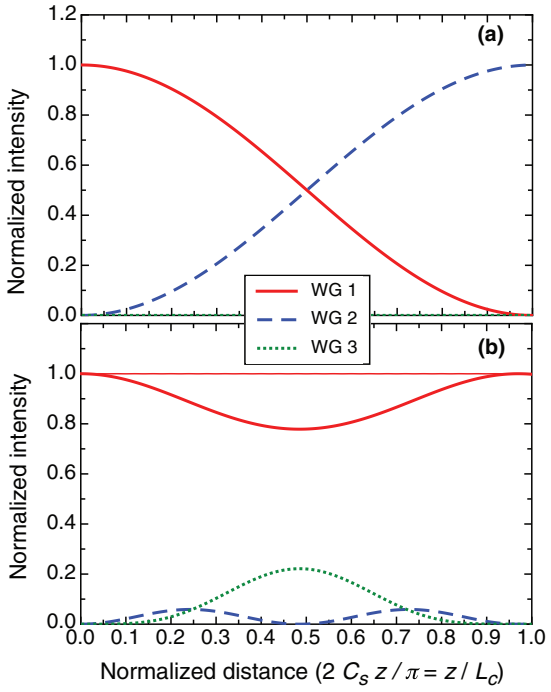

FIG. 2. (Color online) Normalized intensities $|A'_j(z)|^2$ as a function of the distance z normalized to the coupling length, as obtained by integration of Eq. (3) for $\Delta\beta = 0$. (a) is for a large distance between WGs 2 and 3 so that $C_p \ll C_s$ and corresponds to a directional coupler composed by WGs 1 and 2. For (b) the distance between WGs 2 and 3 is reduced so that $C_p = 5C_s$ (thick lines), and WG 1 becomes transparent, in analogy to the EIT effect. The thin solid line in (b) is for the limit of a stronger coupling between WGs 2 and 3, $C_p = 100C_s$.

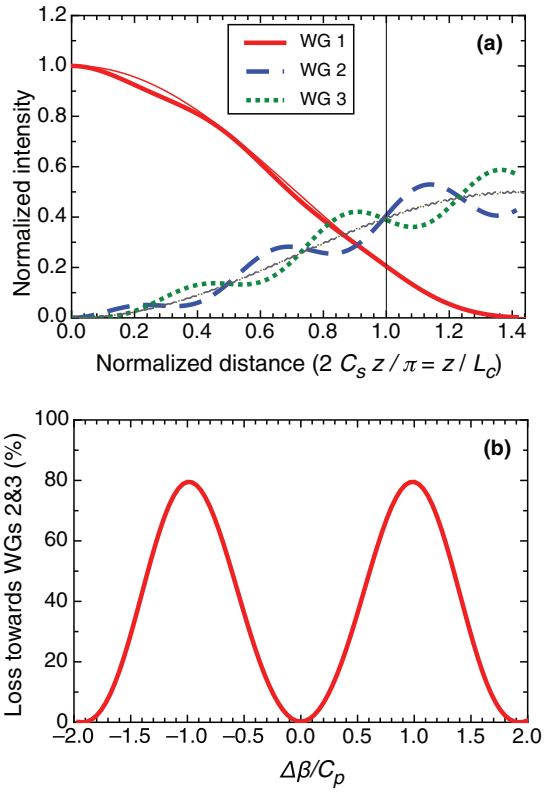

FIG. 3. (Color online) (a) Normalized intensities $|A'_j(z)|^2$ as a function of the distance z normalized to the coupling length as obtained by integration of Eq. (3) or (5) for $\Delta\beta = C_p$. The thick lines are for $C_p = 5C_s$, and the thin lines are for $C_p = 100C_s$. (b) Dependence of the loss from WG 1 due to coupling towards WGs 2 and 3 as a function of $\Delta\beta$ for $C_p = 5C_s$ and $z = L_c = \pi/(2C_s)$. The points at $\Delta\beta = \pm C_p$ give the two Autler-Townes resonances.

not complete. However, the theory predicts a complete transfer for a propagation distance by a factor $\sqrt{2}$ longer. This is easily understood by considering the factor $1/\sqrt{2}$ imposed on the coupling constant C_s by the diagonalization of the strong-coupling portion of the Hamiltonian matrix in (5). Finally, we represent in Fig. 3(b) the spectrum of the light transfer ratio from WG 1 to the other two waveguides as a function of the detuning $\Delta\beta$. The point at $\Delta\beta = 0$ corresponds to the case of EIT discussed above, while the two peaks give the two Autler-Townes resonances at $\Delta\beta = \pm C_p$. Again, the two calculated peak values for the light transfer at the two resonances reach only roughly 80% since they are taken at a distance $z = L_c$ (as in the experiments below) rather than at $z = \sqrt{2}L_c$.

III. EXPERIMENTAL RESULTS AND DISCUSSIONS

Experimental demonstrations of the optical analogies to the EIT and Autler-Townes effect have been performed using the waveguide structures represented in Figs. 1(a) and 1(b). The coupled waveguides have been realized by photoinduction using our experimental platform based on lateral illumination described in detail in [27]. This technique has been successfully exploited for photoinducing waveguides confined in one or two dimensions [32]. More recently, it was used for demonstrating an optical analog to the STIRAP effect [27] and realizing a new concept for broadband beam splitters based on adiabatic passage [14]. With this technique, the image of the desired structure is imprinted onto a 532-nm cw control beam using a reflection-type spatial light modulator (SLM) based on nematic liquid crystals. The structured control beam is then imaged by two crossed cylindrical lenses on a 23-mm-long, weakly Ce doped $Sr_{0.61}Ba_{0.39}Nb_2O_6$ (SBN) crystal. This illumination, combined with a bias electric field E_0 applied parallel to the crystallographic c axis of SBN, enables a photorefractive process leading to a redistribution of charges in the crystal. The result of this redistribution is a local change of the refractive index via the Pockels effect. The design of the refractive index contrast is mastered by adjusting the static field E_0 and the shape and intensity of the control beam. Therefore an easy reconfiguration of the structures can be made by changing the image sent to the SLM and/or the intensity of the control beam. This is used to modify the distance d between WGs 2 and 3 to demonstrate the EIT-like behavior and to modify the longitudinal propagation constant β_1 in WG 1 to demonstrate the optical analog to the Autler-Townes effect. Indeed, as illustrated in Fig. 1(b), by changing the gray level of the image of WG 1 sent to the SLM, the corresponding control beam intensity is changed and so is β_1 and the related refractive index contrast of WG 1. Finally, the photoinduced structure is probed by a low-power

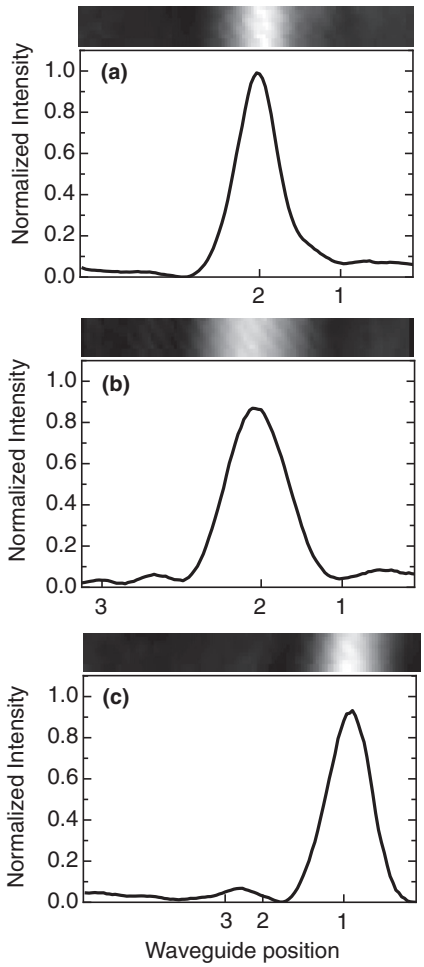

FIG. 4. Output probe beam intensity images and profiles (a) for a two-waveguide directional coupler and for the case of three waveguides with (b) $d = 36\ \mu$m and (c) $d = 2.4\ \mu$m. The case in (c) corresponds to the EIT-like behavior of the three coupled WGs.

633-nm He-Ne laser beam coupled to WG 1 at the input face of the crystal. Its intensity after propagation through the crystal (output face) is imaged on a CCD camera. The change of the propagation constant β upon change of the gray level for the control light has been calibrated experimentally using a Mach-Zehnder interferometer on this probe wave.

We first describe the experiments that provide the analogy of the waveguide structures to the EIT behavior. As discussed theoretically in Sec. II, in this case the structure is composed of three identical WGs [Fig. 1(a)] with no detuning ($\Delta\beta = 0$), which corresponds in quantum physics to three atomic levels mutually coupled by resonant coherent light fields [$\Delta = 0$; see Fig. 1(c)]. In the experiments the WG width is equal to 7.2 μm, and its length L is equal to the 23-mm crystal length. The refractive index contrast of the three waveguides is $\Delta n = 9 \times 10^{-5}$. The distance between WGs 1 and 2 is fixed at 13.2 μm, whereas the distance d between WGs 2 and 3 is being varied. The distance between WGs 1 and 2 is chosen such that WGs 1 and 2 form a directional coupler with $L = L_c$ and $C_{1,2} = 0.6\ \text{cm}^{-1}$. This means that in the absence of WG 3 all the light injected in WG 1 at the input of the crystal should be integrally transferred to WG 2 at the output.

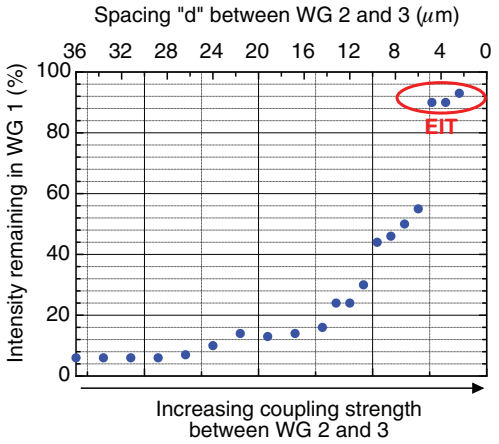

FIG. 5. (Color online) Experimental results demonstrating the optical analogy to EIT. The intensity remaining in WG 1 is plotted for different values of spacing d between WGs 2 and 3 while the spacing between WGs 1 and 2 is kept constant and equal to 13.2 μm.

The experimental results are shown in Figs. 4 and 5. Figure 4 presents the probe beam intensity images and profiles at the end of the propagation in the device for three different cases. Figure 5 represents the intensity remaining in WG 1 at the sample output as a function of d. If there is no WG 3 [Fig. 4(a)], as expected, almost all the light injected in WG 1 is captured by WG 2. If the third waveguide is added sufficiently far apart [$d = 36\ \mu$m; Fig. 4(b)], essentially no perturbation of the propagation occurs, and the output profile is similar to that in Fig. 4(a), in accordance with the theory [Fig. 2(a)]. When d is decreased, coupling between WGs 2 and 3 starts to occur, and some light is transferred back to WG 1, as shown in Fig. 5. For these intermediate cases, the light is partly coupled in WG 2 and in WG 3 while some light remains in WG 1. This corresponds to a three-waveguide asymmetric coupler. Finally, when d becomes sufficiently small [see Fig. 4(c) and the three rightmost points on Fig. 5], almost all the light initially injected in WG 1 remains in this WG at the end of the propagation, as expected theoretically [Fig. 2(b)]. In other words, the presence of WG 3 very close to WG 2 prevents the coupling between WGs 1 and 2. This makes WG 1 transparent, in analogy to the EIT effect.

The evolution of the light distribution among the waveguides in the above cases can be better visualized by performing numerical simulations using a beam propagation method (BPM). Figure 6(a) shows the ratio of intensity which is expected to remain in WG 1 as a function of d, as obtained by BPM calculations under the experimental conditions. A very good qualitative agreement with the experimental results of Fig. 5 can be recognized. Figures 6(b) and 6(c) visualize the corresponding evolution of the propagating wave intensity in the two limiting cases, $d = 36\ \mu$m and $d = 2.4\ \mu$m, respectively. In the first case WG 1 is lossy towards WG 2. In contrast, for $d = 2.4\ \mu$m the light remains confined in WG 1, as found experimentally. Note that for these conditions we have $C_p \approx 3.4\ \text{cm}^{-1}$. This value was estimated numerically using BPM simulations by considering the spatial beating of the wave amplitude between WG 2 and WG 3 when only these waveguides are present. Furthermore, experimental

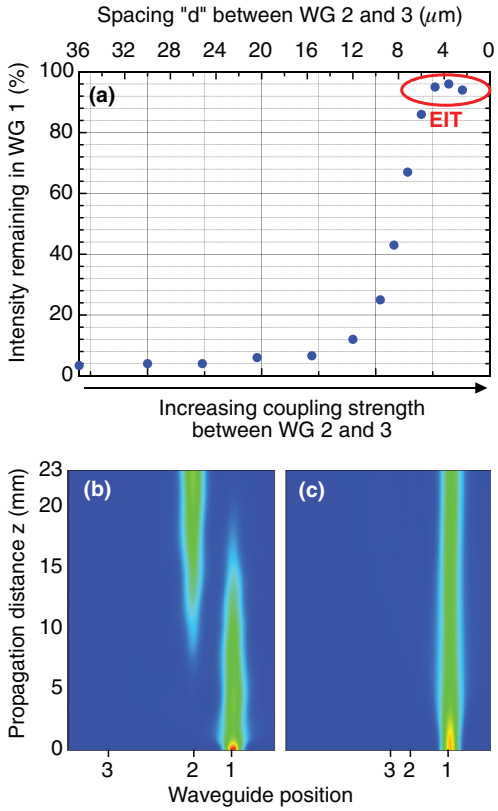

FIG. 6. (Color online) (a) Intensity remaining in WG 1 as a function of d calculated with BPM simulations. Simulation of the probe beam intensity evolutions in z for (b) $d = 36$ μm and (b) for $d = 2.4$ μm. Numerical parameters are taken in accordance with the experimental ones.

verification by counting the observed numbers of beats during the dynamic evolution of WGs 2 and 3 confirms the above value within a 20% error margin.

Next, we demonstrate experimentally the Autler-Townes functionalities of the three-waveguide system. Here the distance d is fixed at 2.4 μm. Therefore, if the WGs are not detuned ($\Delta\beta = 0$), we are facing the case of the EIT-like effect discussed above. To demonstrate the Autler-Townes effect we

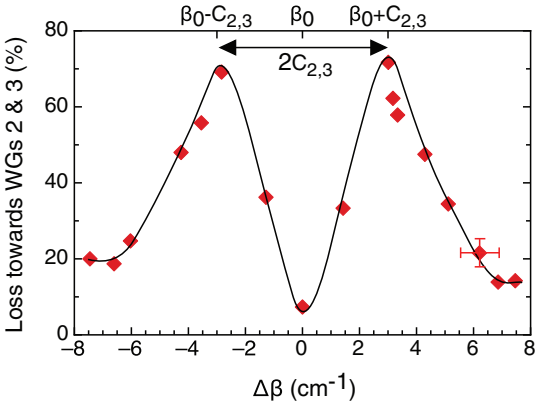

FIG. 7. (Color online) Experimental demonstration of the Autler-Townes effect illustrated by measuring the loss from WG 1 towards WGs 2 and 3 vs the detuning $\Delta\beta$ of the first WG.

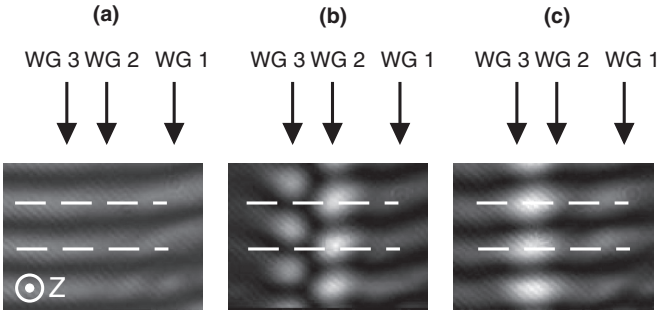

FIG. 8. Probe beam interferograms (a) in the absence of WGs and for (b) the left and (c) the right resonances of Fig. 7, showing an antisymmetric (symmetric) state for the left (right) resonance.

introduce a detuning of the longitudinal propagation constant of WG 1 ($\beta_1 = \beta_0 + \Delta\beta$). This is done by modifying the gray level of the image used for creating WG 1, as explained above. This is now analogous to an atomic Λ system where the first two levels (Ψ_1 and Ψ_2) are weakly coupled by a coherent light field slightly off resonance and where states Ψ_2 and Ψ_3 are strongly coupled by a resonant light field.

Different structures are tested for various detunings $\Delta\beta$. The experimental results are summarized in Fig. 7, which, similar to Fig. 3(b), gives the intensity loss from WG 1 towards WGs 2 and 3 as a function of $\Delta\beta$. The central point, for which $\Delta\beta = 0$, corresponds to EIT, and almost all the light injected in WG 1 remains in this WG, as in Fig. 4(a). By increasing $|\Delta\beta|$ the loss is maximized for two particular values symmetric to the origin, where $|\Delta\beta|$ has been measured to be 3 ± 0.5 cm^{-1}, which is in good agreement with the above value of C_p. Therefore, in agreement with the theoretical expectations, the two Autler-Townes resonances are found for $\Delta\beta = \pm C_p = \pm C_{2,3}$. Note also that, experimentally, the maximum loss is slightly less than 80%, as expected for $L = L_c$ and from the discussion in Sec. II.

Finally, to get an additional proof of the involved effects we have investigated the form of the optical modes associated with the two resonances in Fig. 7. This is done by observing the superposition of the light exiting from WGs 2 and 3 with a plane wave on a Mach-Zehnder-type interferometer. Figure 8(a) is obtained in the unperturbed crystal when there are no waveguides and constitutes the reference. For the left resonance in Fig. 7 ($\Delta\beta = -3$ cm^{-1}) the interferogram reveals that the light fields in WGs 2 and 3 are mutually out of phase [Fig. 8(b)] and correspond to an antisymmetric state (supermode). In contrast, for the right resonance ($\Delta\beta = +3$ cm^{-1}) we find a symmetric state, as seen in Fig. 8(c). This corresponds to the expected symmetries of the two dressed states [see Eq. (4)] and proves the power of optics for the direct visualization of such states.

IV. CONCLUSION

We have investigated theoretically and demonstrated experimentally an optical analogy to the EIT and Autler-Townes effect from quantum physics by using photoinduced coupled waveguides. The experimental results are in good agreement with the theoretical expectations and numerical simulations. The waveguide structures have been realized using an

experimental platform that permits easy modification of the implemented photoinduced optical structures. We have first used the adaptability of our experimental system to tune the coupling between WGs 2 and 3, allowing us to steer the output port of the signal injected in WG 1. This can be port 2 or port 1, with no modification of WGs 1 and 2, in analogy with EIT. Furthermore, by detuning the propagation constant β_1 in WG 1 with respect to the ones in WGs 2 and 3, we have directly demonstrated an analogy to the Autler-Townes splitting. This effect can potentially be used as a tunable mode converter. For practical purposes the response time of the process is presently limited by the photorefractive response speed associated with the creation, modification, and reconfiguration of the waveguides, which is rather slow (typically, a few seconds) for the SBN crystal being used. However, this speed can be increased by several orders of magnitude by using faster photorefractive materials such as $Sn_2P_2S_6$ [33] or by taking advantage of the interband photorefractive effect [34]. Alternatively, in the case of sufficiently intense pulse light, the mutual properties of the waveguides might be instantaneously modified by means of the optical Kerr effect.

ACKNOWLEDGMENTS

This work has been supported by Bulgarian National Science Fund Grant No. DMU-03/103 and by the Lorraine region through the Contrat de Projets Etats-Région (CPER), project "Matériaux, Energie, Procédés, Produits."

[1] L. De Broglie, Comptes Rendus **177**, 507 (1923).
[2] E. Schrödinger, Naturwissenschaften **23**, 807 (1935).
[3] S. Longhi, Phys. Rev. A **71**, 065801 (2005).
[4] R. Khomeriki and S. Ruffo, Phys. Rev. Lett. **94**, 113904 (2005).
[5] S. Longhi, J. Opt. B **7**, L9 (2005).
[6] F. Dreisow, A. Szameit, M. Heinrich, S. Nolte, A. Tünnermann, M. Ornigotti, and S. Longhi, Phys. Rev. A **79**, 055802 (2009).
[7] H. Suchowski, D. Oron, A. Arie, and Y. Silberberg, Phys. Rev. A **78**, 063821 (2008).
[8] H. Suchowski, V. Prabhudesai, D. Oron, A. Arie, and Y. Silberberg, Opt. Express **17**, 12731 (2009).
[9] E. Paspalakis, Opt. Commun. **258**, 30 (2006).
[10] S. Longhi, Phys. Rev. E **73**, 026607 (2006).
[11] S. Longhi, G. Della Valle, M. Ornigotti, and P. Laporta, Phys. Rev. B **76**, 201101 (2007).
[12] Y. Lahini, F. Pozzi, M. Sorel, R. Morandotti, D. N. Christodoulides, and Y. Silberberg, Phys. Rev. Lett. **101**, 193901 (2008).
[13] S. Longhi, Opt. Lett. **32**, 1791 (2007).
[14] C. Ciret, V. Coda, A. A. Rangelov, D. N. Neshev, and G. Montemezzani, Opt. Lett. **37**, 3789 (2012).
[15] S. Longhi, Laser Photonics Rev. **3**, 243 (2009).
[16] S. E. Harris, J. E. Field, and A. Imamoglu, Phys. Rev. Lett. **64**, 1107 (1990).
[17] K.-J. Boller, A. Imamoglu, and S. E. Harris, Phys. Rev. Lett. **66**, 2593 (1991).
[18] M. Fleischhauer, A. Imamoglu, and J. P. Marangos, Rev. Mod. Phys. **77**, 633 (2005).
[19] D. D. Smith, H. Chang, K. A. Fuller, A. T. Rosenberger, and R. W. Boyd, Phys. Rev. A **69**, 063804 (2004).
[20] Q. Xu, S. Sandhu, M. L. Povinelli, J. Shakya, S. Fan, and M. Lipson, Phys. Rev. Lett. **96**, 123901 (2006).
[21] Y.-F. Xiao, X.-B. Zou, W. Jiang, Y.-L. Chen, and G.-C. Guo, Phys. Rev. A **75**, 063833 (2007).
[22] X.-S. Song, F. Xu, and Y.-Q. Lu, Opt. Lett. **36**, 4434 (2011).
[23] S.-Y. Chiam, R. Singh, C. Rockstuhl, F. Lederer, W. Zhang, and A. A. Bettiol, Phys. Rev. B **80**, 153103 (2009).
[24] P. Ginzburg and M. Orenstein, Opt. Express **14**, 11312 (2006).
[25] P. Ginzburg, A. Hayat, V. Vishnyakov, and M. Orenstein, Opt. Express **17**, 4251 (2009).
[26] S. H. Autler and C. H. Townes, Phys. Rev. **100**, 703 (1955).
[27] C. Ciret, V. Coda, A. A. Rangelov, D. N. Neshev, and G. Montemezzani, Phys. Rev. A **87**, 013806 (2013).
[28] A. Yariv, IEEE J. Quantum Electron. **9**, 919 (1973).
[29] W.-P. Huang, J. Opt. Soc. Am. A **11**, 963 (1994).
[30] N. Vitanov, M. Fleischhauer, B. Shore, and K. Bergmann, Adv. At. Mol. Opt. Phys. **46**, 55 (2001).
[31] S. E. Harris, Phys. Today **50**(7), 36 (1997).
[32] M. Gorram, V. Coda, P. Thévenin, and G. Montemezzani, Appl. Phys. B **95**, 565 (2009).
[33] T. Bach, M. Jazbinsek, G. Montemezzani, P. Günter, A. A. Grabar, and Y. M. Vysochanskii, J. Opt. Soc. Am. B **24**, 1535 (2007).
[34] G. Montemezzani, P. Rogin, M. Zgonik, and P. Günter, Opt. Lett. **18**, 1144 (1993).